# UAV RGB excess green mapping of dense but low-diversity mangrove stands on Pagerungan Besar Island, Indonesia

[1]Husamah H., [1]Abdulkadir Rahardjanto, [1]Atok M. Hudha, [1]Ludwick S. Romadoni, [2]Aryo Widyantopo, [2]Retno Anggraeni

[1] Department of Biology Education, Faculty of Teacher Training and Education, Universitas Muhammadiyah Malang, 65144 East Java, Indonesia; [2] Safety, Health and Environment Department, Kangean Energy Indonesia Ltd, 12940 Jakarta, Indonesia. Corresponding author: H. Husamah, e-mail: usya_bio@umm.ac.id

**Abstract.** Mangrove monitoring on small islands requires methods that are accurate at the stand level yet feasible for rapid surveys. This study assessed mangrove community structure and canopy closure on Pagerungan Besar Island (Sapeken Islands, Sumenep Regency, East Java, Indonesia) using ground-based plots and hemispherical photography, and evaluated Unmanned Aerial Vehicles-Red-Green-Blue (UAV RGB) imagery processed with the excess green (ExG) index for density mapping. Eleven mangrove species (four families) were recorded, with *Rhizophora mucronata* Lam. dominating the sheltered North Station (2,600 ind $ha^{-1}$) and *Rhizophora stylosa* Griff. the wave-exposed South Station (2,500 ind $ha^{-1}$). Canopy closure indicated dense to very dense stands (86.8% North; 74.9% South), while diversity contrasted strongly (H' = 1.85 North; 0.50 South) due to pronounced southern dominance (D = 0.68). Correspondence analysis (CA) separated stations along a substrate-wave exposure gradient, revealing zonation between back-mangrove and pioneer zones. In contrast, UAV-based classification (ExG resampled to 10 cm $pixel^{-1}$) underestimated density, classifying 88.2% (North) and 94.1% (South) of the area as sparse. These findings support integrated field-UAV monitoring for island scales, but show that density estimation in heterogeneous canopies likely requires native-resolution processing and/or complementary active sensors.
**Key Words**: mangrove, UAV, excess green, canopy closure, small islands.

**Introduction**. Mangrove forests are among the most valuable coastal ecosystems, providing shoreline stabilization, nursery habitats for fisheries, and major contributions to "blue carbon" storage that supports climate regulation (Rahardjanto et al 2021; Sidik et al 2023; Choudhary et al 2024; Wibowo et al 2024, 2025; Bajahmoum & Almaghamsi 2025). In archipelagic countries such as Indonesia, mangroves also function as natural infrastructure for small islands, where exposure to waves, tidal currents, and storm surges can rapidly reshape shorelines and threaten settlements and livelihoods (Blankespoor et al 2017; Latumahina & Susilawati 2024; Husamah et al 2025). However, mangrove ecosystems remain vulnerable to multiple pressures, including land-use change, coastal development, and resource exploitation, which collectively drive deforestation and degradation and reduce the long-term capacity of mangroves to deliver ecosystem services (Nurwidodo et al 2023; Tran et al 2024; Gunawan et al 2025; Ngo et al 2025). These challenges make consistent, spatially explicit monitoring essential, not only to detect changes in areal extent but also to track structural condition and community composition as indicators of ecosystem health.

Monitoring approaches have therefore expanded from conventional plot-based vegetation inventories to remote sensing products. Field surveys provide species-level identification and robust ecological indices, but they are time-consuming and spatially limited, especially in fragmented island settings. Satellite-based mapping offers broad coverage, yet moderate spatial resolution can be problematic in narrow coastal fringes and mixed land-water pixels (Lawley et al 2016; Ramdiah et al 2018; Matyukira & Mhangara 2024; Rahardjanto et al 2024; Wu et al 2025; Zheng et al 2025). As an alternative, small unmanned aerial vehicles (UAVs) equipped with Red-Green-Blue (RGB) sensors have emerged as a practical tool for rapid, high-resolution coastal mapping. UAV photogrammetry can generate detailed orthomosaics, and simple vegetation indices derived from RGB channels, such as the excess green (ExG) index, are increasingly used to delineate vegetation cover efficiently (Morgan et al 2022; Kovanič et al 2023; Aierken et al 2024; Maes 2025). In principle, these products can support operational monitoring by local stakeholders because they are relatively low-cost and can be repeated frequently.

Despite these advances, a key methodological gap remains: UAV RGB indices are often applied for mapping mangrove extent, but their reliability for estimating stand density and representing canopy complexity is less certain, particularly in heterogeneous mangrove mosaics and under strong tidal, substrate, and shadow effects. Classification outcomes can be sensitive to preprocessing choices (e.g., resampling, threshold selection) and may underrepresent structural attributes that are critical for management decisions, such as canopy closure, zonation, and dominance patterns (Budi et al 2025; Budiarto & Dewanto 2025; Duan et al 2025). For small islands where management actions frequently target specific zones (front/pioneer vs back-mangrove), the ability to integrate vegetation structure with spatial mapping is especially important (Ghorbanian et al 2022; Astarika 2024; Bakar et al 2024; Casal et al 2024). Pagerungan Besar Island (Sapeken, Sumenep Regency, East Java) represents a relevant case: an earlier baseline study documented mangrove communities in the área (Hidayah & Andriyani 2019; Rahardjanto et al 2020; Nugraha & Luthfi 2024), yet updated evidence is needed to describe current community structure and to evaluate practical monitoring tools that can be used for repeated assessment.

Building on this need, this paper advances a monitoring paradigm that treats structural ground-truth (density, zonation, and canopy closure) as a required validation layer for UAV RGB mapping, rather than assuming that RGB-derived indices alone can represent stand condition in complex canopies. Accordingly, this study investigated mangrove community structure and canopy condition at two contrasting stations on Pagerungan Besar Island and evaluated the performance of UAV-based RGB mapping for density classification. Specifically, we aimed to: (1) quantify species composition and density, and calculate ecological indices (diversity, richness, evenness, dominance) using plot inventories; (2) validate forest structural condition using hemispherical photography-derived canopy closure; (3) explore species-station associations and zonation patterns using correspondence analysis (CA) (McGarigal et al 2000) in relation to substrate and exposure gradients; and (4) compare ground-truth indicators of density with UAV RGB classification based on the ExG index. This work contributes (1) an updated, station-scale ecological baseline for mangroves on Pagerungan Besar Island, including quantitative indices and zonation interpretation relevant for conservation and restoration planning; and (2) an applied evaluation of UAV RGB-ExG mapping for density-related monitoring in small-island mangroves, highlighting conditions under which low-cost UAV workflows may misestimate structural condition and therefore require careful validation or methodological refinement.

## Material and Method

***Research location***. This research was conducted on Pagerungan Besar Island, Sumenep Regency, East Java, Indonesia (central coordinate approximately 6.9568°S, 115.9182°E, WGS84). The study focused on two distinct mangrove stations characterized by differing environmental conditions (Figure 1). The North Station is located in the back-mangrove zone (≈ 6.9527°S, 115.9250°E), exhibiting a sheltered environment with a heterogeneous substrate composed of deep mud interspersed with coral patches. In contrast, the South Station is situated in the coastal fringe zone (≈ 6.9606°S, 115.9271°E), characterized by a muddy sand substrate and exposed to direct wave action and tidal currents (Figure 1).

### Data collection

***Vegetation survey***. Mangrove community structure was assessed using a stratified purposive sampling method. A total of four observation plots, each measuring 10x10m, were established to represent the dominant vegetation zones: three plots in the North Station and one plot in the South Station. Within each plot, all mangrove trees were identified to the species level following standard taxonomic keys. The number of individuals was recorded to calculate species density (ind $ha^{-1}$) and community indices.

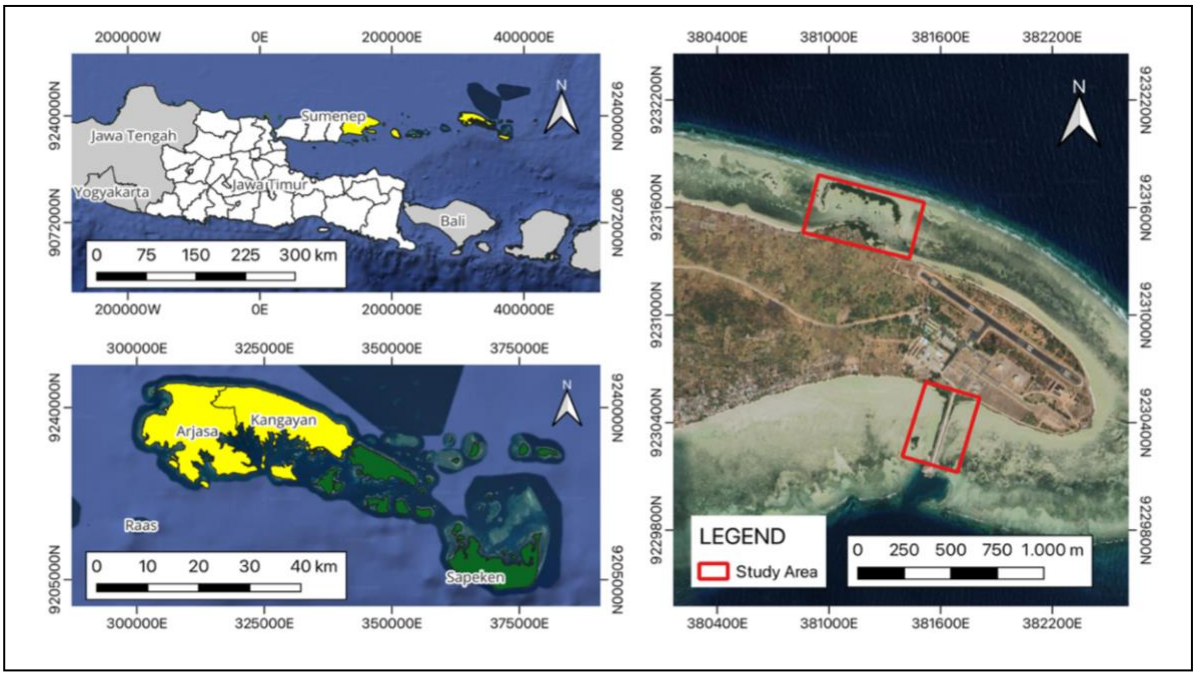


Figure 1. Map of the study area in Pagerungan Besar Island showing the location of North and South sampling stations.

***Drone image acquisition and processing***. Aerial imagery was acquired using a DJI Phantom 4 quadcopter equipped with a standard onboard RGB camera (1/2.3″ CMOS sensor). Flight missions were conducted at an altitude of 80 meters to ensure consistent ground sampling distance (GSD). The raw images were processed using photogrammetric software to generate a high-resolution orthomosaic with a native spatial resolution of 2.22 cm $pixel^{-1}$. The orthomosaic was used to compute the ExG on a per-pixel basis using the standard formulation ExG = 2G - R - B, where R, G, and B represent the red, green, and blue band values, respectively. For density mapping, the ExG raster was classified into four canopy-density classes using fixed numeric thresholds (T1 = 0.05, T2 = 0.12, T3 = 0.20. As shown in Table 1, to align with the operational mapping workflow, the ExG raster was additionally resampled to 10 cm $pixel^{-1}$ before classification, and the same thresholds were applied to the resampled product.

Table 1

ExG thresholds used for UAV-based canopy-density classification

| *Class* | *Canopy density label* | *ExG range (thresholds)* |
|---|---|---|
| 1 | Sparse | ExG < 0.05 |
| 2 | Moderate | 0.05 ≤ ExG < 0.12 |
| 3 | Dense | 0.12 ≤ ExG < 0.20 |
| 4 | Very dense | ExG ≥ 0.20 |

Note: ExG is the excess green index, a popular, simple RGB-based vegetation index used to distinguish green vegetation.

To estimate mangrove density, the orthomosaic was converted into the ExG vegetation index. For the purpose of this spectral analysis, the orthomosaic was resampled to a resolution of 10 cm pixel$^{-1}$ to optimize processing efficiency during classification. The vegetation cover was then classified into density classes based on ExG thresholding values.

Hemispherical Photography. To validate canopy density from the ground, hemispherical photography was acquired at the center of each plot using a fisheye lens. The images were analyzed to calculate the percentage of canopy closure, serving as a ground-truth proxy for forest density.

***Data analysis***. The structure of the mangrove community was analyzed using several standard ecological indices.

The Shannon–Wiener diversity index was calculated as:

$$H' = -\sum p_i ln\ p_i$$

Where:
$H'$ = Shannon–Wiener diversity index,
$p_i$ = proportion of individuals belonging to species $i$, calculated as $p_i = n_i/N$, $n_i$ is the number of individuals of species $i$,
$N$ = total number of individuals in the community,
$S$ = total number of species present in the sample. The summation was performed across all species present in the sample ($i = 1 \dots S$), and the natural logarithm ($ln$ ) was used in the calculation (Shannon & Weaver 1949; Nolan & Callahan 2006).

Pielou's evenness index was calculated as:

$$J' = \frac{H'}{ln\, S}$$

Where:
$\boldsymbol{E}$ = Pielou's evenness index,
$H'$ = Shannon–Wiener diversity index,
$S$ = total number of species (Pielou 1966; Ricotta & Avena 2003).

Margalef's richness index was calculated as:

$$R = \frac{S - 1}{ln\, N}$$

Where:
$R$ i = Margalef's richness index,
$S$ = the total number of species,
$N$ = total number of individuals, and the natural logarithm (*ln*) was used (Margalef 1963; Gamito 2010).

Margalef's richness index is sometimes denoted as $D_{Mg}$ or *d i*n ecological studies.

Simpson's dominance index was calculated using the following formula:

$$\boldsymbol{D} = \sum \boldsymbol{p}_i^2$$

Where:
$D$ = Simpson's dominance index,
$p_i$ = proportion of individuals belonging to species $i$, calculated as $p_i = n_i/N$, where $n_i$ is the number of individuals of species $i$ and $N$ is the total number of individuals of all species (Simpson 1949).

In this study, higher $D$ values indicate greater species dominance and lower diversity within the community.

To visualize the association between mangrove species and sampling stations, CA was performed using statistical software. Species abundance data were log-transformed using log(x+1) before analysis to stabilize variance. The results were presented in a biplot to identify the spatial segregation of species assemblages across sampling stations. In CA, inertia refers to the amount of variation in the species-by-station matrix explained by a given axis, analogous to the proportion of variance explained in principal component analysis. Therefore, axes with higher inertia represent the major ecological gradients structuring the assemblages.

## Results and Discussion

***Taxonomic composition and species density***. A total of 11 mangrove species belonging to 4 families (*Rhizophoraceae, Lythraceae, Acanthaceae, Primulaceae*) were identified across the study area. The detailed taxonomic composition and distribution of these species are presented in Table 2.

Table 2

Taxonomic composition and distribution of mangrove species

| *Class* | *Order* | *Family* | *Species* |
|---|---|---|---|
| Magnoliopsida | Malpighiales | Rhizophoraceae | *Rhizophora mucronata* Lam. |
| | | | *Rhizophora stylosa* Griff. |
| | | | *Bruguiera gymnorrhiza* (L.) Lam. |
| | | | *Bruguiera sexángula* (Lour.) Poir. |
| | | | *Bruguiera parviflora* (Roxb.) Wight & Arn. ex Griff. |
| | Myrtales | Lythraceae | *Sonneratia alba* Sm. |
| | | | *Sonneratia ovata* Backer |
| | | | *Pemphis acidula* J. R. Forst & G. Forst. |
| | Lamiales | Acanthaceae | *Avicennia lanata* Ridl. |
| | | | *Avicennia alba* Blume |
| | Ericales | Primulaceae | *Aegiceras corniculatum* (L.) Blanco |

The spatial distribution of these species across the island highlights a distinct separation between the two stations, as illustrated in the Species Distribution Map (Figure 2). The North Station exhibits a complex mix of species, whereas the South Station is mono-dominant.

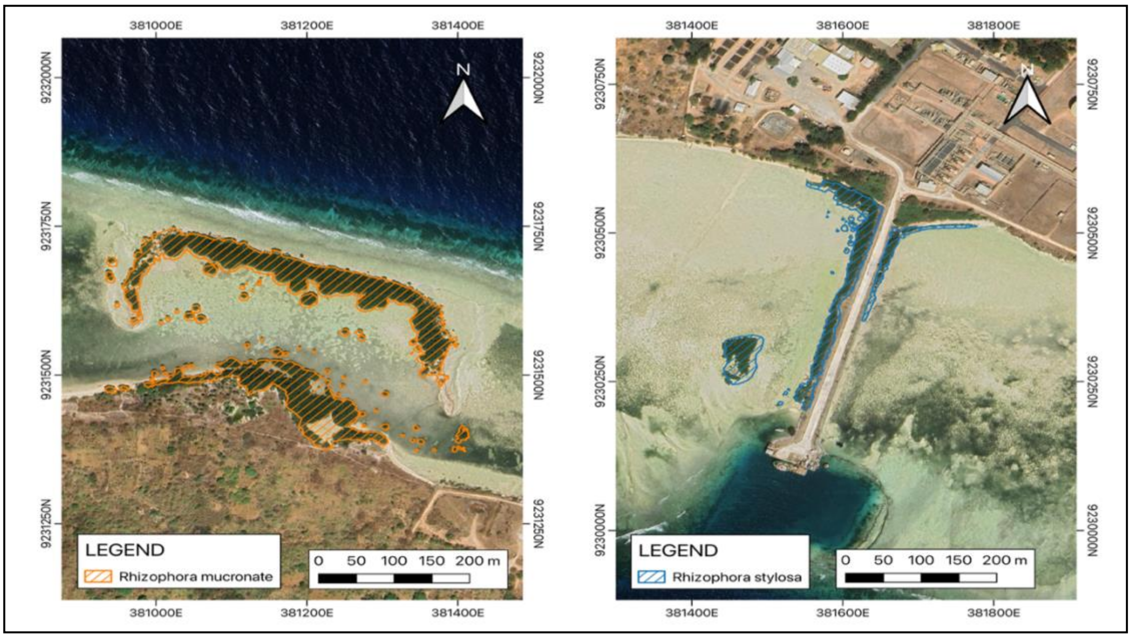


Figure 2. Spatial distribution of dominant mangrove species at the North and South Stations (Source: Researchers' personal data).

The ecological health of the community is further summarized in Table 3. The North Station supports a much higher species richness and diversity compared to the South, which is characterized by high dominance (D = 0.68).

Table 3

Ecological indices comparison between North and South Stations

| Ecological index | North station | South station |
|---|---|---|
| Richness index (R) | 1.84 | 0.31 |
| Diversity index (H') | 1.85 | 0.50 |
| Evenness index (E) | 0.84 | 0.72 |
| Dominance index (D) | 0.28 | 0.68 |

Quantitative analysis of vegetation density confirmed that both stations support "Very Dense" mangrove forests. The North Station recorded a total density of 2,600 ind ha$^{-1}$, dominated by *Rhizophora mucronata* (1,333 ind ha$^{-1}$). The South Station recorded 2,500 ind ha$^{-1}$, dominated almost exclusively by *Rhizophora stylosa* (2,000 ind ha$^{-1}$) (Figure 3).

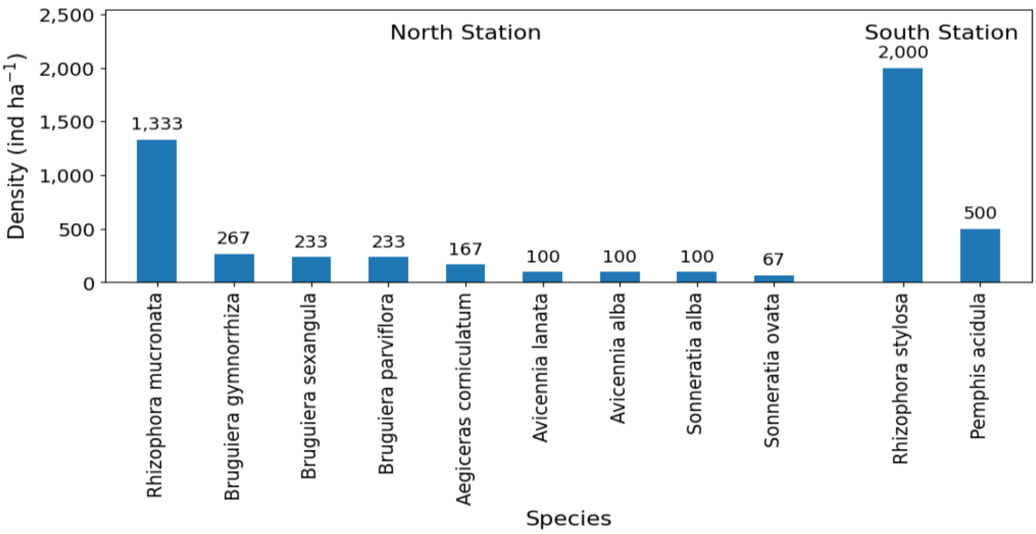


Figure 3. Vegetation analysis and mangrove species density.

***Spatial zonation and substrate influence***. The CA biplot revealed a sharp ecological gradient between the two stations (Figure 4). The analysis demonstrated an extremely high goodness-of-fit, with the first two dimensions explaining 99.7% of the total inertia. Dimension 1 accounted for 97.5% of the variance, highlighting the critical role of environmental factors in driving species segregation.

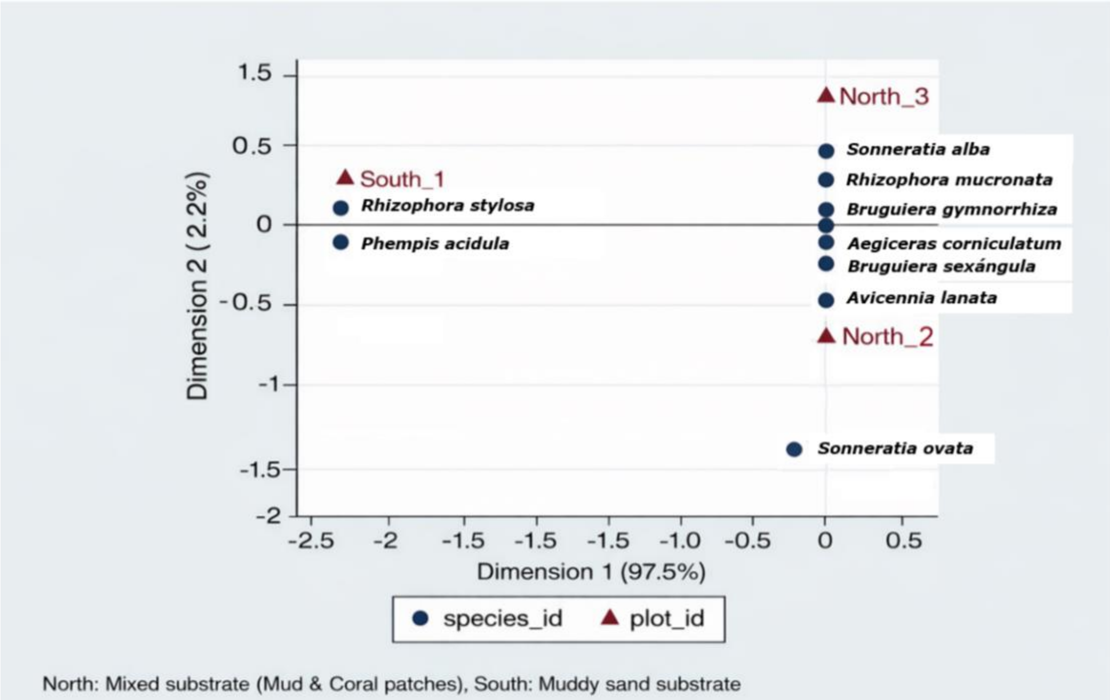


Figure 4. Correspondence analysis Biplot showing the distinct association between mangrove species and sampling plots driven by substrate heterogeneity (CA input summary: No. Species in CA matrix: 11; No. Plots: 4 [North = 3; South = 11).

The plots from the North Station clustered tightly on the positive axis of Dimension 1. This grouping reflects a consistent community structure supported by a heterogeneous substrate. As detailed in Table 4, the North Station consists of deep mud interspersed with coral patches. This habitat mosaic facilitates high species richness (S = 9) by providing suitable niches for both mud-specialists (*R. mucronata* & *Bruguiera* spp.) and species adapted to firmer substrates (*Sonneratia alba*).

Conversely, the South Station formed an isolated cluster on the negative axis, exclusively associated with *R. stylosa* and *P. acidula*. The dominance of these species indicates a "front-mangrove" environment with muddy sand substrate and higher wave energy, which selects for specific pioneer species capable of withstanding physical stress.

Table 4

Environmental characteristics of the study sites

| *Environmental parameter* | *North Station* | *South Station* |
| --- | --- | --- |
| Substrate type | Deep mud mixed with coral patches | Muddy sand |
| Inundation type | Daily tidal inundation | Tidal + wave splash |
| Wave exposure | Low (sheltered back-reef) | High (open coastal fringe) |
| Dominant vegetation zone | Mid/back mangrove zone | Front/pioneer mangrove zone |

***Methodological discrepancy***

***Drone and ground truth***. A significant finding of this study is the discrepancy between drone-derived density (ExG) and ground-truth data. While field surveys and hemispherical photography (Canopy Closure > 74%) confirmed the forest as "Very Dense," the drone analysis classified 88% of the North area and 94% of the South area as "Sparse Mangrove" (Table 5).

Table 5

Comparison of mangrove density estimation methods

| *Parameter* | *Method* | *Metric / Classification* | *North Station* | *South Station* |
|---|---|---|---|---|
| Field survey | Plot counting (10×10 m) | Tree density (ind $ha^{-1}$) | 2,600 (Very dense) | 2,500 (Very dense) |
| Canopy cover | Hemispherical photography | Canopy closure (%) | 86.8% (Very dense) | 74.9% (Dense) |
| Drone analysis | RGB Orthomosaic (ExG Index)* | Sparse mangrove area (%) | 88.2% | 94.1% |
| | | Moderate mangrove area (%) | 8.5% | 4.2% |
| | | Dense mangrove area (%) | 3.3% | 1.7% |

This underestimation is visualized in the Density Maps (Figure 5), where the area appears largely sparse despite the dense reality on the ground.

This discrepancy is attributed to the methodological decision to resample the imagery to 10 cm $pixel^{-1}$. Although the DJI Phantom 4 captured data at a high resolution (2.22 cm $pixel^{-1}$), the downsampling process introduced a "mixed pixel" effect. In a complex mangrove canopy, a single 10x10 cm $pixel^{-1}$ likely aggregates the spectral values of leaves, branches, and background water/mud, thereby diluting the greenness signal (ExG). Furthermore, the RGB-based index lacks the sensitivity to detect the dense understory vegetation (*Bruguiera* saplings and *Aegiceras* shrubs) that contributes significantly to the total density observed in the field. This suggests that while cost-effective RGB drones are suitable for mapping the areal extent, accurate density estimation in heterogeneous forests requires processing at native resolution or the integration of active sensors, Light Detection and Ranging (LiDAR) to account for vertical stratification.

The field results indicate that both stations support high mangrove density, yet their community structure differs substantially. The sheltered North Station showed higher richness and diversity, which is consistent with the presence of multiple microhabitats created by a heterogeneous substrate (deep mud mixed with coral patches) and low wave exposure. Such habitat mosaics can provide suitable niches for taxa with different rooting strategies and tolerances, allowing co-occurrence of *Rhizophora*, *Bruguiera*, *Avicennia*, *Sonneratia*, and associated shrubs. By contrast, the coastal fringe South Station was strongly dominated by *Rhizophora stylosa* and *Pemphis acidula*, reflecting a pioneer front-mangrove setting where stronger hydrodynamic energy and muddy-sand substrate filter the community to a narrower set of stress-tolerant species.

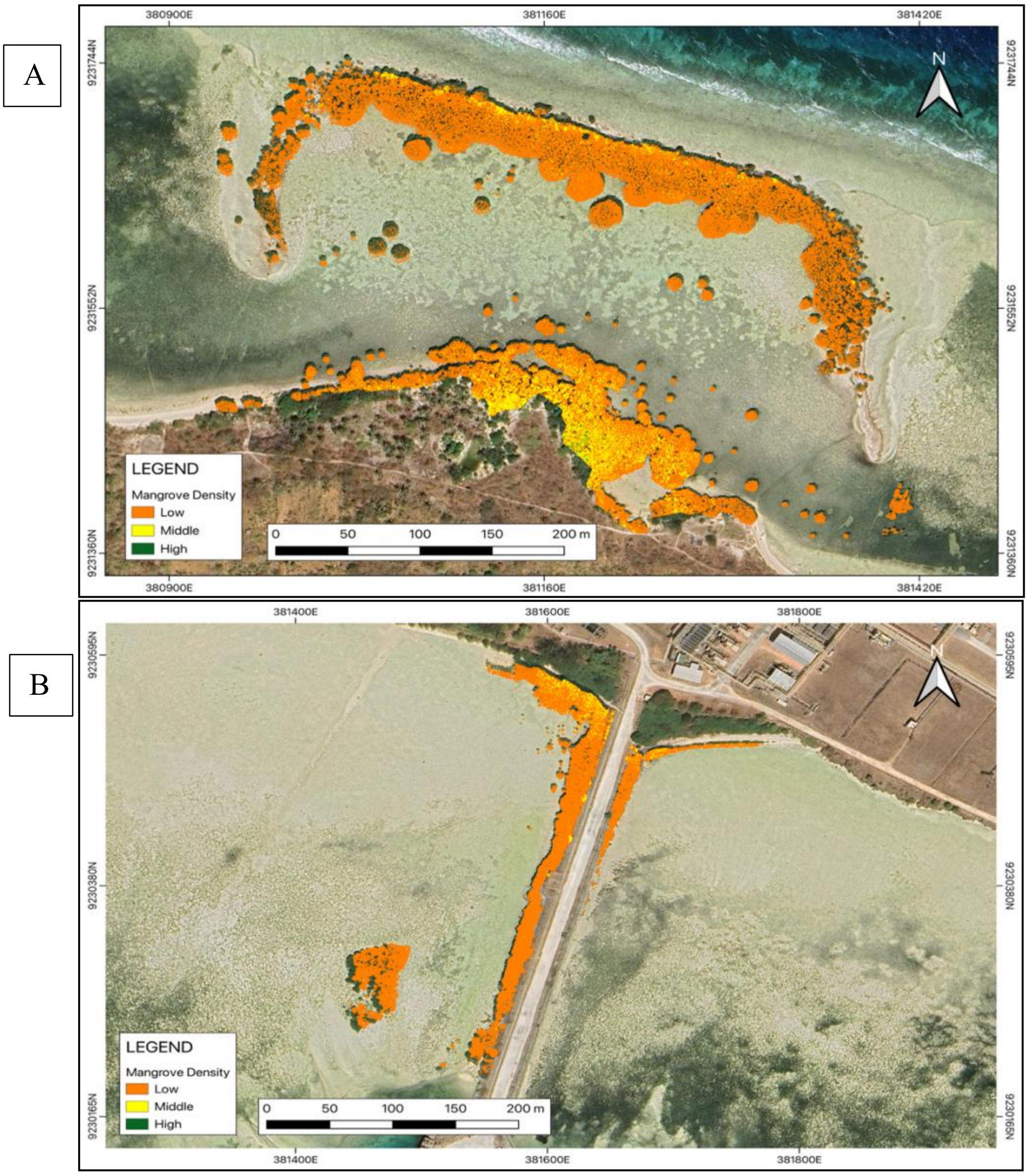


Figure 5. Comparison of mangrove density maps derived from drone ExG index (resampled to 10 cm): (A) North Station showing fragmented density, and (B) South Station showing sparse classification (Source: Researchers' personal data).

To improve future monitoring and reduce the underestimation observed with RGB-ExG classification, subsequent surveys should integrate complementary tools that better capture canopy complexity. Incorporating UAV multispectral sensors (red-edge/NIR) would allow indices such as NDVI/red-edge metrics that are less sensitive to shadows and mixed substrate-water reflectance than RGB-only ExG. In parallel, using 3D structural products from UAV surveys (SfM point clouds/canopy height models, and UAV LiDAR where available) would provide direct proxies of stand structure (height and canopy complexity) that can be linked more robustly to density and canopy closure. Operationally, applying RTK/PPK GNSS and GCPs for repeated surveys and moving beyond fixed thresholds to OBIA or machine-learning classifiers that combine spectral and textural features would strengthen classification reliability in heterogeneous small-island mangrove mosaics.

From a conservation perspective, the coexistence of a diverse back-mangrove zone and a simplified fringe zone highlights the importance of maintaining landscape-level heterogeneity on small islands. Back-mangrove areas with higher species richness may enhance resilience through functional complementarity and can underpin long-term ecosystem services such as shoreline stabilization and carbon sequestration (Rahman et al

2021; Woroniecki et al 2023; Ferreira et al 2024). At the same time, dominance-driven communities at the fringe can still provide critical coastal protection but may be more sensitive to additional disturbances because reduced diversity can limit recovery pathways following extreme events or human pressures (see Table 6) (Jordan & Fröhle 2022; Sacatelli et al 2023; DiPetto et al 2025; Meraj et al 2025).

Table 6

Ecological implications of dominance-driven fringe mangroves versus diverse back-mangrove stands (Pagerungan Besar Island)

| *Aspect* | *Dominance-driven fringe (e.g., South Station)* | *More diverse back-mangrove (e.g., North Station)* | *Implication for management* |
|---|---|---|---|
| Community pattern | Few species dominate; low diversity | Higher richness/diversity | Interpret resilience differently across zones |
| Coastal protection function | Often high (dense roots/stems at shoreline) | Moderate-high (depends on stand structure) | Protect shoreline-front stands as priority buffers |
| Sensitivity to disturbance | Potentially higher (limited diversity → fewer recovery pathways) | Potentially lower (higher functional redundancy) | Reduce additional stressors in fringe; maintain connectivity |
| Recovery after extreme events | Can be slower if dominant species is impacted | More pathways for recruitment/compensation | Plan post-disturbance restoration by zone |
| Monitoring focus | Track dominant species condition + canopy gaps | Track composition shifts + recruitment across microhabitats | Use zone-specific indicators and sampling designs |

The UAV comparison demonstrates a key operational limitation: RGB-based ExG mapping can be highly sensitive to spatial resolution and preprocessing choices when used to infer density rather than extent. In this study, resampling the orthomosaic to 10 cm pixel$^{-1}$ likely increased spectral mixing between foliage and non-vegetated background (water, mud, shadows), leading to systematic dilution of greenness signals and classification into lower density classes. Moreover, an RGB index primarily captures upper-canopy greenness and may not represent understory contributions to stand density, which were captured in plot inventories and indirectly reflected in canopy closure measurements. These findings suggest that UAV RGB workflows are most reliable for delineating mangrove cover and broad structure at native resolution, while density estimation in heterogeneous stands should either avoid coarse resampling, incorporate object-based approaches, or combine passive imagery with structural information (e.g., LiDAR-derived canopy height models) (Jurado et al 2022; Lassalle et al 2023; Mai et al 2025; Qin et al 2025; Zhai et al 2025).

Taken together, the integrated field-UAV workflow provides an updated baseline for Pagerungan Besar Island and supports practical monitoring on small islands. Future monitoring should prioritize consistent acquisition protocols, retain native spatial resolution during classification when structural metrics are needed, and expand plot replication in exposed fringe zones to strengthen inference on community gradients and restoration priorities.

Taken together, the integrated field-UAV workflow provides an updated baseline for Pagerungan Besar Island and offers a practical, scalable monitoring template for Indonesian coastal management, including institutional contexts such as Malang, East Java, where universities and local agencies can serve as regional hubs for capacity building and rapid ecological assessment. In particular, combining plot inventories and hemispherical photography with low-cost UAV RGB mapping enables (i) species- and structure-resolved baselines for restoration planning, and (ii) repeatable, high-resolution shoreline monitoring that can be implemented by local stakeholders after short training. Future monitoring should prioritize consistent acquisition protocols, retain native spatial resolution during classification when structural metrics are needed, and expand plot replication in exposed fringe zones to strengthen inference on community gradients and restoration priorities.

For Indonesian government implementation, we recommend: (1) institutionalize a standard operating procedure (SOP) for small-island mangrove monitoring that couples field plots + canopy closure with UAV surveys (including tidal-stage and illumination controls) to improve comparability across districts; (2) invest in local capacity and shared equipment pools (UAV units, GNSS/RTK, and processing workstations) through provincial/DLH and university partners (e.g., regional hubs in East Java such as Malang) to reduce cost barriers and ensure continuity; (3) require ground-truth validation when UAV products are used for density/condition reporting (not only extent), and promote higher-fidelity tools (multispectral or 3D structural products) for heterogeneous canopies where RGB indices underperform; and (4) link monitoring outputs to actionable programs—zoning-based protection of fringe buffers, targeted enrichment in back-mangrove areas, and performance-based evaluation for restoration funding—so that monitoring directly informs coastal protection, livelihoods, and blue-carbon outcomes.

**Conclusions**. Mangrove stands on Pagerungan Besar Island were classified as dense to very dense based on plot inventories and hemispherical canopy closure, with clear ecological contrasts between a heterogeneous, species-rich back-mangrove North Station and a wave-exposed, low-diversity pioneer South Station. Correspondence analysis indicated strong zonation linked to substrate and wave exposure. UAV RGB-ExG classification at a resampled resolution of 10 cm pixel$^{-1}$ substantially underestimated density, highlighting the importance of processing at native resolution and validating structure-related metrics with ground data. These findings support the use of integrated field-UAV approaches for rapid small-island monitoring and for informing conservation and restoration planning. For local management, the zonation pattern suggests prioritizing strict protection of the wave-exposed fringe as a coastal buffer while directing restoration and enrichment actions to more diverse back-mangrove areas, with monitoring protocols calibrated to avoid underestimating canopy condition.

**Acknowledgements.** The authors thank Universitas Muhammadiyah Malang (UMM) and the Institute for Research and Community Service and the Bureau of Research and Cooperation of UMM for field and logistical support. Thanks also to Kangean Energy Indonesia Ltd for the facilities and funding provided. Funding information: Internal Research Schema with contract number E.2.a/275.10/RPK/UMM/2025.

**Conflict of interest.** The authors declare that there is no conflict of interest.

**References**

Aierken N., Yang B., Li Y., Jiang P., Pan G., Li S., 2024 A review of unmanned aerial vehicle based remote sensing and machine learning for cotton crop growth monitoring. Computers and Electronics in Agriculture 227:109601.
Astarika R., 2024 Spatial analysis of mangrove cover change and land suitability for its rehabilitation in Tanjungpinang City, Riau Islands Province, Indonesia. AACL Bioflux 17(6):2905-2921.
Bajahmoum E. A., Almaghamsi A., 2025 Physicochemical degradation of Avicennia marina mangrove soils in the Red Sea : implications for coastal ecosystem services. Frontiers in Soil Science 5:1621591.
Bakar N. A., Jaafar W. S. W. M., Maulud K. N. A., Kamarulzaman A. M. M., Saad S. N. M., Mohan M., 2024 Monitoring mangrove-based blue carbon ecosystems using UAVs: a review. Geocarto International 39(1):2405123.
Blankespoor B., Dasgupta S., Lange G-M., 2017 Mangroves as a protection from storm surges in a changing climate. Ambio A Journal of Environment and Society 46(4):478-491.
Budi M., He T., Song D-X., Wang C., 2025 Mapping 30 m fractional tree cover using PlanetScope-3B images and Landsat-8 spectral-texture data for a case study of

different forest types in Indonesia. Geo-spatial Information Science 2025:1-32.
Budiarto R., Dewanto B. G., 2025 Unmanned aerial vehicles for assessing biomass and carbon stocks in mangrove forests: a systematic review. Sustainable Futures 10:101425.
Casal G., Trégarot E., Cornet C. C., McCarthy T., van der Geest M., 2024 A cost-effective method to map mangrove forest extent, composition, and condition in small islands based on Sentinel-2 data: Implications for management. Ecological Indicators 159:111696.
Choudhary B., Dhar V., Pawase A. S., 2024 Blue carbon and the role of mangroves in carbon sequestration: Its mechanisms, estimation, human impacts and conservation strategies for economic incentives. Journal of Sea Research 199:102504.
DiPetto G. R., Bilkovic D. M., Sloey T. M., Yando E. S., Walters E. L., 2025 Future-oriented coastal protection: The utility of living shorelines under changing climatic conditions. Nature-Based Solutions 100285.
Duan M., Sanchez-Azofeifa A., Abdulmajeed M., Turner D., Buckingham K., Odari A., Mtwana J., Kipkoech S., Kasraee N., 2025 Aboveground carbon estimation in a mangrove ecosystem using UAV-based remote sensing and machine learning. Ecological Indicators 178:113950.
Ferreira A. C., Ashton E. C., Ward R. D., Hendy I., Lacerda L. D., 2024 Mangrove biodiversity and conservation: setting key functional groups and risks of climate-induced functional disruption. Diversity 16(7):423.
Gamito S., 2020 Caution is needed when applying Margalef diversity index. Ecological Indicators 10(2):550-551.
Ghorbanian A., Ahmadi S. A., Amani M., Mohammadzadeh A., Jamali S., 2022 Application of artificial neural networks for mangrove mapping using multi-temporal and multi-source remote sensing imagery. Water 14(2):244.
Gunawan H., Basyuni M., Subarudi S., Suharti S., Kustanti A., Wahyuni T., Arifanti V. B., Yeny I., Affandi O., Sugiarti S., 2025 Empowering conservation: the transformative role of mangrove education in Indonesia’s climate strategies. Forest Science and Technology 21(4):374-396.
Hidayah Z., Andriyani L., 2019 Carbon stock analysis of mangrove ecosystems in Paliat Island Sumenep East Java. In: IOP Conference Series: Earth and Environmental Science 276(1):012034.
Husamah H., Rahardjanto A., Lestari N., Permana T. I., Hudha A. M., 2025 Relationship of Environmental Literacy and Action Competence for Sustainability: Indonesian Islamic Junior-Senior High Students. International Journal of Environmental Impact 8(4):727-73.
Jordan P., Fröhle P., 2022 Bridging the gap between coastal engineering and nature conservation? Journal of Coastal Conservation 26(2):4.
Jurado J. M., López A., Pádua L., Sousa J. J., 2022 Remote sensing image fusion on 3D scenarios: A review of applications for agriculture and forestry. International Journal of Applied Earth Observation and Geoinformation 112:102856.
Kovanič Ľ., Topitzer B., Peťovský P., Blišťan P., Gergeľová M. B., Blišťanová M., 2023 Review of Photogrammetric and Lidar Applications of UAV. Applied Sciences 13(11):6732.
Lassalle G., Ferreira M. P., Cué La Rosa L. E., Scafutto R. D. M., Filho C. R. S, 2023 Advances in multi- and hyperspectral remote sensing of mangrove species: A synthesis and study case on airborne and multisource spaceborne imagery. ISPRS Journal of Photogrammetry and Remote Sensing 195:298-312.
Latumahina S. F., Susilawati S., Mangrove forest health assessment on small island in Maluku, Indonesia. International Journal on Advanced Science, Engineering and Information Technology 14(6):2031-2038.
Lawley V., Lewis M., Clarke K., Ostendorf B., 2016 Site-based and remote sensing methods for monitoring indicators of vegetation condition: an Australian review. Ecological Indicators 60:1273-1283.
Maes W. H., 2025 Practical guidelines for performing UAV mapping flights with snapshot sensors. Remote Sensing 17(4):606.

Mai X., Li Q., Xu W., Deng S., Wang W., Wu W., Zhang W., Wang Y., 2025 Estimation of mangrove aboveground carbon using integrated UAV-LiDAR and satellite data. Sustainability 17(18):8211.
Margalef R., 1963 On certain unifying principles in ecology. The American Naturalist 97(897):357-374.
Matyukira C., Mhangara P., 2024 Advances in vegetation mapping through remote sensing and machine learning techniques: a scientometric review. European Journal of Remote Sensing 57(1):2422330.
Meraj G., Abouleish M. Y., Ali T., Hashimoto S., Marazi A., Chakrabortty R., Singh S. K., Kanga S., Almazroui M., Bhuyan M. S., 2025 Middle Eastern mangroves at the arid limit ( Red Sea and Arabian / Persian Gulf ): eco- biophysical dynamics, blue-carbon MRV, climate-risk pathways, and governance for resilient restoration - a comprehensive review. Frontiers in Marine Science 12:1695426.
Morgan R. G., Hodgson M. E., Wang C. R., Schill S., 2022 Unmanned aerial remote sensing of coastal vegetation: a review. Annals of GIS 28(3):385-399.
Ngo T. H., Fang Q., Liang Z., Hu H., Ma D., 2025 Integrating the unknowns into cumulative human impact assessment identifies extensive areas of mangroves in Southeast Asia under human pressure. Global Change Biology 31(7):e70338.
Nolan K. A., Callahan J. E., 2006 Beachcomber biology: The Shannon-Weiner Species Diversity Index. Proceedings of the 27th Workshop/Conference of the Association for Biology Laboratory Education (ABLE). pp. 334-338.
Nugraha W. A., Luthfi S. A., 2024 High diversity of mangrove ecosystem on the North Coast of Bangkalan, East Java, Indonesia. Egyptian Journal of Aquatic Biology and Fisheries 28(4):2131-2146.
Nurwidodo N., Ibrohim I., Sueb S., Husamah H., 2023 "Let's transform!": a systematic literature review of science learning in COVID-19 pandemic era. Eurasia Journal of Mathematics, Science and Technology Education 19(2):em2224.
Pielou E. C., 1966 The Measurement of Diversity in Different Types of Biological Collections. Journal of Theoretical Biology 13:131-144.
Qin Q., Dai W., Wang X., 2025 Super resolution for mangrove UAV remote sensing images. Symmetry 17(8):1250.
Rahardjanto A., Husamah H., Hadi S., Rofieq A., Wahyono P., 2020 Community structure, diversity, and distribution patterns of sea cucumber (Holothuroidea) in the coral reef area of Sapeken Islands, Sumenep Regency, Indonesia. AACL Bioflux 13(4):1795-1811.
Rahardjanto A., Husamah H., Sabilah F., 2024 Environmental risk perception of prospective biology teachers in Indonesia in the pandemic era. Journal of Education and Learning 18(3):930-937.
Rahardjanto A., Tosiyana V. R., Husamah H., Miharja F. J., 2020 Diversity of molluscs in the mangrove forest area of Cengkrong Beach-Trenggalek. AIP Conference Proceedings 2231(1):040075.
Rahman M. M., Zimmer M., Ahmed I., Donato D., Kanzaki M., Xu M., 2021 Co-benefits of protecting mangroves for biodiversity conservation and carbon storage. Nature Communications 12(1):3875.
Ramdiah S., Mayasari R., Husamah H., Fauzi A., 2018 The effect of TPS and PBL learning models to the analytical ability of students in biology classroom. Asia-Pacific Forum on Science Learning and Teaching 19(2):18.
Ricotta C., Avena G., 2003 On the relationship between Pielou's evenness and landscape dominance within the context of Hill's diversity profiles. Ecological Indicators 2(4):361-365.
Sacatelli R., Kaplan M., Carleton G., Lathrop R. G., 2023 Coastal forest dieback in the northeast USA: potential mechanisms and management responses. Sustainability 15(8):6346.
Shannon C. E., Weaver W., 1948 A mathematical theory of communication. Urbana: University of Illinois Press, 1.
Sidik F., Lawrence A., Wagey T., Zamzani F., Lovelock C. E., 2023 Blue carbon: a new paradigm of mangrove conservation and management in Indonesia. Marine Policy

147:105388.
Simpson E. H., 1949 Measurement of diversity. Nature 163:688.
Tran T. V., Reef R., Zhu X., 2024 Long-term changes of mangrove distribution and its response to anthropogenic impacts in the Vietnamese Southern Coastal Region. Journal of Environmental Management 370:122658.
Wibowo F. A. C., Alkornea D., Chanan M., 2025 Conservation of soil physical and chemical properties by application of compost and biochar in Tambakrejo Village, Malang Regency. Jurnal Pengelolaan Sumberdaya Alam dan Lingkungan Hidup 15(3):435-447
Wibowo F. A. C., Chanan M., Pratama S. I., 2024 Lead level analysis in roots and leaves of mangrove plants *Ceriops tagal* and *Rhizophora apiculata* in Clungup mangrove conservation. Media Konservasi 29(2):137-147.
Woroniecki S., Spiegelenberg F. A., Chausson A., Turner B., Key I., Md. Irfanullah H., Seddon N., 2023 Contributions of nature-based solutions to reducing people's vulnerabilities to climate change across the rural Global South. Climate and Development 15(7):590-607.
Wu Y., Lu C., Wu K., Gao W., Yang N., Lin J., 2025 Advancements and trends in mangrove species mapping based on remote sensing: A comprehensive review and knowledge visualization. Global Ecology and Conservation 57:e03408.
Zhai C., Zhang Y., Wu Y., Shen X., 2025 Accurate evaluation of urban mangrove forest health considering stand structure indicators based on UAVs. Forests 16(7):1168.
Zheng P., Han D., Liu J., Xu B., Fang P., Huang S., Liu W., Chen S., 2025 A new approach for monitoring spatial and temporal changes in forest types in subtropical regions with sample migration and multi-source remote sensing data. Geo-spatial Information Science 1-29.

Received: 23 December 2025. Accepted: 25 January 2026. Published online: 11 March 2026.
Authors:
Husamah, Department of Biology Education, Faculty of Teacher Training and Education, Universitas Muhammadiyah Malang, Raya Tlogomas Street, No. 246 Malang, 65144 East Java, Indonesia, e-mail: usya_bio@umm.ac.id
Abdulkadir Rahardjanto, Department of Biology Education, Faculty of Teacher Training and Education, Universitas Muhammadiyah Malang, Raya Tlogomas Street, No. 246 Malang, 65144 East Java, Indonesia, e-mail: abdkadir@umm.ac.id
Atok Miftachul Hudha, Department of Biology Education, Faculty of Teacher Training and Education, Universitas Muhammadiyah Malang, Raya Tlogomas Street, No. 246 Malang, 65144 East Java, Indonesia, e-mail: dwis@umm.ac.id
Ludwick Satria Romadoni, Department of Biology Education, Faculty of Teacher Training and Education, Universitas Muhammadiyah Malang, Raya Tlogomas Street, No. 246 Malang, 65144 East Java, Indonesia, e-mail: ludwicksatriaromadoni@webmail.umm.ac.id
Aryo Widyantopo, Safety, Health and Environment Deparment, Kangean Energy Indonesia Ltd, The Convergence Indonesia 29th, HR. Rasuna Said Street, 12940 South Jakarta, Jakarta, Indonesia, e-mail: info@kangean-energy.com
Retno Anggraeni, Safety, Health and Environment Department, Kangean Energy Indonesia Ltd, The Convergence Indonesia, 29th, HR. Rasuna Said Street, South Jakarta, Jakarta 12940, Indonesia, e-mail: info@kangean-energy.com

How to cite this article:
Husamah H., Rahardjanto A., Hudha A. M., Romadoni L. S., Widyantopo A., Anggraeni R., 2026 UAV RGB excess green mapping of dense but low-diversity mangrove stands on Pagerungan Besar Island, Indonesia. AACL Bioflux 19(2):468-481.